

Parametric amplification in single-walled carbon nanotube nanoelectromechanical resonators

Chung-Chiang Wu and Zhaohui Zhong*

*Department of Electrical Engineering and Computer Science, University of Michigan,
Ann Arbor, MI 48109, USA.*

*Corresponding author: zzhong@umich.edu

ABSTRACT

The low quality factor (Q) of Single-walled carbon nanotube (SWNT) resonators caused by thermalelastic dissipation, has limited their sensitivity in sensing application. To this end, we employ the technique of parametric amplification by modulating the spring constant of SWNT resonators at twice the resonant frequency, and achieve 10 times Q enhancement. The highest Q obtained at room temperature is around ~ 700 , which is 3-4 times better than previous Q record reported for doubly-clamped SWNT resonators. Furthermore, efficient parametric amplification is found to only occur in the catenary vibration regime. Our results open up the possibility to employ light-weight and high- Q carbon nanotube resonators in single molecule and atomic mass sensing.

Keywords: carbon nanotube, nanoelectromechanical resonators, parametric amplification
quality factor, nonlinearity,

With the progress in lithography and material synthesis, nanoelectromechanical systems (NEMS) [1-2] have attracted great interests over the last decade. They can operate at higher frequency with lower power consumption and are expected to have excellent sensitivities in ultra-small mass [3-6] and force sensing [7]. For application in mass spectrometry, a mass sensitivity below a single Dalton (1 Da= 1 AMU) has been predicted theoretically [8]. In principle, the amount of detected mass is determined by measuring the shift in resonant frequency. Generally, the minimum detectable mass (Δm) of NEM resonators can be expressed as [1, 3] $\Delta m = 2 \frac{m_{eff}}{Q}$, where m_{eff} is the effective mass of the resonator. For better mass sensitivity, one would prefer a resonator with the lowest mass and the highest possible Q . To this end, SWNT resonator stands out with one of the highest Young's modulus [9] and the lightest effective mass and is considered as a promising candidate [10-11] to achieve this ultimate goal. m_{eff} for nanotube ($\sim 10^{-18}$ g) is at least three orders of magnitude less than those of other resonators. Unfortunately, the mass sensitivity of SWNT resonators [12-15] is impeded by a poor quality factor. Previous studies showed that as structures shrink down to nanometer size scale, the surface effects resulting from the increasing surface-to-volume ratio (R) would limit the quality factor [1, 16]. More importantly, strain in nanostructure will generate local temperature difference, leading to irreversibly heat flow along local temperature gradients and inducing the thermalelastic dissipation [1, 16-17]. As the ultimate 1D nanostructure, SWNT resonator's room temperature Q is limited at several dozens. One solution to improve nanotube resonator's sensitivity is to utilize the concept of parametric amplification for Q enhancement.

Parametric resonance is excited by a time-varying modulation of a system parameter. A common example of parametric resonance is a pendulum, with the length of the cord changing

with time. If the length decreases when the pendulum is in the lower position and increases in the upper position, oscillations of the pendulum will build up. The first application of parametric amplification in a mechanical resonance system was demonstrated by Rugar and Grütter [18]. In their work, parametric amplification in a mechanical cantilever was obtained by periodically modulating the spring constant on the basis of gate capacitive coupling. Thereafter, numerous studies based on parametric amplification in MEMS resonators have been conducted by many other schemes, for example, exploiting stress via piezoelectric electromechanical coupling [19] or a Lorentz force [20]. Here, we demonstrate parametric amplification in SWNT resonators by modulating the spring constant through a simple electrostatic gate coupling scheme.

To understand parametric amplification in SWNT resonators, we start from the equation of motion. Without loss of generality, we modeled the SWNT resonator as a driven harmonic oscillator with a damping term and a time-varying spring constant. The equation of motion is expressed as [18]

$$m \frac{d^2 x}{dt^2} + \frac{m\omega_0}{Q} \frac{dx}{dt} + [k_0 + k_p(t)]x = F(t) \quad (1)$$

, where x is the displacement of the nanotube , $F(t)$ is the external driving force, Q is the quality factor, ω_0 is the resonant frequency, k_0 is the unperturbed spring constant, and k_p is the modulated spring constant created by electrostatic coupling, written as $k_p = \Delta k \sin 2\omega_0 t$. M , k_0 , and ω_0 are related by $k_0 = m\omega_0^2$. The parametric amplification will lead to a vibration amplitude gain (G) given by [18]

$$G = \left[\frac{\cos^2 \phi}{(1 + V_p/V_t)^2} + \frac{\sin^2 \phi}{(1 - V_p/V_t)^2} \right]^{1/2} \quad (2)$$

, where ϕ is the phase between the driving and pumping signals, V_t is the threshold voltage determined by the system parameters, and V_p is the pumping voltage for parametric amplification. From equation (2), it is expected that the gain will increase as V_p approaches V_t when an appropriate ϕ is satisfied.

To experimentally verify the parametric amplification, we fabricated SWNT resonators using the one-step direct transfer technique reported previously [21]. Briefly, suspended SWNTs were grown across pillars on a transparent quartz substrate by the chemical vapor deposition (CVD) [22-24], while pre-designed electrodes were fabricated on a separate device substrate using conventional lithography. The transfer of suspended SWNTs to the device substrate was implemented by simply bringing the two substrates into contact by using a contact aligner (Karl Suss MJB-3). For a typical device, the source (S) and drain (D) electrodes are 2 μm wide, separated by 3 μm , 50 nm Au is used as contact metal, and the distance between nanotube and the bottom gate (G) is 1 μm . Detail parameters of similar SWNT resonators can be found in our previous work [24].

To actuate and detect resonance signals of our SWNT resonators, we employed frequency modulation (FM) mixing technique [25] instead of amplitude modulation (AM) method [26] in our measurement setup, as shown in Figure 1(a). For external FM modulation, a small signal from a lock-in amplifier (Stanford Research SR830) at low frequency (616.3Hz) was sent to the RF signal generator (Agilent 8648B). The FM signal was then sent to the source electrode to actuate the resonance and the mixing current from the drain electrode was measured by the lock-in amplifier. To achieve parametric amplification, a second AC voltage (pumping voltage, V_p) from second RF signal generator (Agilent 8648C) at twice the resonant frequency $2f_o$ was coupled with the DC gate voltage through a bias-T, and was applied to the gate electrode

to modulate the spring constant of the nanotube. We note that the FM mixing technique was chosen as the detection technique because of its better noise-rejection in comparison to the AM method and the background current is zero (an advantage in detecting resonance) [25]. In addition, since the spring constant of the nanotube is modulated by applying V_p , the vibrational noise caused by pumping signal may degrade the performance of parametric amplification if the noise-sensitive AM method is used.

To demonstrate parametric amplification, our SWNT resonator was measured in a vacuum chamber at pressure below 10^{-4} torr and $\delta V_{sd} = 20$ mV was applied to drive the nanotube. The mixing current as a function of driving frequency at different pumping voltages are plotted in Figure 1(b). At $V_p = 0$, we observe a nanotube resonance at $f_0 = 23.1$ MHz with a poor Q of 24 ± 1 . As we increase the V_p at $2f_0$ frequency, resonance peak amplitude is significantly enhanced and peak width is reduced, indicating a Q enhancement. The quality factors are extracted by fitting the experimental data of Figure 1(b) with [25]:

$$I(\omega) = \frac{2\omega(\omega^2 - \omega_0^2 - \frac{\omega_0^2}{Q})(\omega^2 - \omega_0^2 + \frac{\omega_0^2}{Q})}{[(\omega_0^2 - \omega^2)^2 + (\frac{\omega_0\omega}{Q})^2]} \quad (3)$$

Fig. 1(c) shows the Q (blue squares) and corresponding gain (Q_p/Q_o) (red triangles) at different V_p . A clear Q enhancement was observed as V_p gradually increases. The maximum enhancement of Q was achieved at $V_p = 25$ mV with $Q=235\pm9$ (blue curve), showing remarkably a 10-fold enhancement compared to the signal without pumping (red curve, $Q=24\pm1$). We further compare our Q value with previous works on doubly-clamped SWNT resonators [12-13, 15, 26-29] in Fig. 1(d). Overall, previous room temperature Q record is around 200, while our highest Q through

parametric amplification is ~ 700 (marked as a star and the resonance signal with fitting curve is shown in inset), showing at least three times improvement.

Next, we examined effects of system parameters on parametric amplification by looking at the DC gate voltage dependence and the AC driving voltage dependence on parametric amplification. Figure 2 (a) and 2(c) show the maximum gains at different DC gate voltages obtained from two SWNT resonators, respectively. On both devices, we consistently observed effective parametric amplification with gain between 2 to 4 at higher DC gate voltages (blue triangles), but no amplification with gain ~ 1 at lower gate voltages (red triangles). To understand this disruption of parametric amplification, we plotted resonant frequency vs. V_g for both resonators in the Figure 2(b) and 2(d), respectively. The resonance frequency is up-shifted at higher potential due to elastic hardening [24, 26], and two vibrational regimes, bending and catenary regimes, are clearly observed [26]. Comparing the gain obtained at different DC gate voltages with the corresponding vibration regimes, we found that efficient parametric amplification only occurs in the catenary regimes for both resonators.

To understand the vibration mode dependent amplification, we refer to the relationship [26] between the resonant frequency and the gate-induced tension (T). When a DC voltage (V_g^{DC}) and a pumping voltage ($V_p \cos 2\omega_o t$) are coupled and applied on the gate electrode, the electrostatic force can be expressed as $F_e = \frac{1}{2}C_g' V_g^{DC^2} + C_g' V_p \cos 2\omega_o t$ by ignoring the higher order term, where C_g' is the derivative of the gate capacitance. As the SWNT resonator is vibrating in the catenary regime, the resonant frequency is proportional to the square root of the gate-induced tension ($f \propto \sqrt{T}$), yielding a linear dependence of the spring constant

modulation on the change in the gate-induced tension ($\Delta k \propto \Delta T$). Because the gate-induced tension is modulated by the electrostatic force at $2f_0$, the nanotube spring constant will also experience this modulating effect at $2f_0$, leading to efficient parametric amplification. On the other hand, in the bending regime, the resonant frequency is proportional to the gate-induced tension ($f \propto T$), suggesting that the spring constant has a parabolic relationship with the gate-induced tension. If V_p at $2f_0$ is applied, the spring constant will be modulated at $4f_0$ instead of at $2f_0$, resulting in poor/no Q enhancement in the bending regime.

We also examined the effect of excitation driving voltage (V_{sd}) on parametric amplification, and the results of maximum gain vs. V_p with different V_{sd} at a fixed DC gate voltage ($V_g = -4$ V) are plotted in Fig. 2(e). The experimental data did not reveal any dependence between maximum gain and V_{sd} when the V_{sd} was increased from 20 mV to 60 mV. This result is consistent with observations from previous work, where no dependence was observed between the gain and V_{sd} [19].

Last, we examine the threshold voltage for parametric amplification (V_t). As shown in Figure 3(a), gain increases sharply with increasing V_p , agreeing with optimum parametric amplification near the threshold voltage. In order to extract V_t from the measurement data, we note that equation (2) is derived under fixed phase lag between driving and pumping. However, our FM technique will introduce a time varying phase lag, and hence the overall gain is an average result due to random phases. Therefore, the average gain using our measurement technique can be written as

$$G = \frac{1}{2\pi} \int_0^{2\pi} G(\phi) d\phi = \frac{1}{2\pi} \int_0^{2\pi} \left[\frac{\cos^2 \phi}{(1 + V_p/V_t)^2} + \frac{\sin^2 \phi}{(1 - V_p/V_t)^2} \right]^{1/2} d\phi \quad (4)$$

Fitting data in Fig. 3(a) with equation (4), we find a $V_t = 0.24$ V at $V_g = -5$ V. We further extract V_t values under various V_g , and plot them in Fig. 3(b) (red squares). To model V_t dependence on V_g , we follow the derivation of Rugar and Grütter [18] and have V_t expressed as $V_t = 2k_0/QV_gC_g''$, where V_g is the DC gate voltage and C_g'' is the second derivative of the gate capacitance. To calculate the theoretical values of V_t , we adopt the cylinder over an infinite plane model for capacitance, $C = \frac{2\pi\epsilon_0 L}{\ln(\frac{2Z}{d})}$, and the results are plotted as blue diamonds in Figure 3(b). The experimental results show good agreement with the theoretical V_t values, suggesting the possibility to predict and control V_t by changing the device geometries and gate coupling. We also notice the deviation from the theoretical V_t at $V_g = -6$ V, and its origin is not clear at this time.

Our results enable the light-weight carbon nanotube as high-Q NEM resonator for single molecule and atomic mass sensing. We also expect the parametric amplification technique can be applied to other low-Q NEM resonators suffering from intrinsic loss mechanisms, such as graphene resonators [30]. The $2f_0$ modulation through electrostatic gating offers a simple technique which can be easily adopted in various device geometries and the flexibility to be integrated with NEMS applications.

Note Added:

Upon the completion of the manuscript, we became aware of a related work published online on Nano Letters [31]. Both works achieve parametric amplification by applying pumping voltages on the gate electrode, but with different measurement schemes and different focuses.

Acknowledgements

The work is supported by the start-up fund provided by the University of Michigan. This work used the Lurie Nanofabrication Facility at University of Michigan, a member of the National Nanotechnology Infrastructure Network funded by the National Science Foundation.

References

- [1] K. L. Ekinci, and M. L. Roukes, *Rev. Sci. Instrum.* **76**, 061101 (2005).
- [2] A. N. Cleland, *Foundations of Nanomechanics* (Springer-Verlag, Berlin 2003).
- [3] K. L. Ekinci, Y. T. Yang, and M. L. Roukes, *J. Appl. Phys.* **95**, 2682 (2004).
- [4] Y. T. Yang *et al.*, *Nano Lett.* **6**, 583 (2006).
- [5] C. Hierold *et al.*, *Sens. Actuators A* **136**, 51 (2007).
- [6] A. K. Naik *et al.*, *Nature Nanotech.* **4**, 445 (2009).
- [7] H. J. Mamin, and D. Rugar, *Appl. Phys. Lett.* **79**, 3358 (2001).
- [8] A. N. Cleland, *New J. Phys.* **7**, 235 (2005).
- [9] A. Krishnan *et al.*, *Phys. Rev. B* **58**, 14013 (1998).
- [10] S. Sapmaz *et al.*, *Phys. Rev. B* **67**, 235414 (2003).
- [11] A. Kis, and A. Zettl, *Philos. Trans. R. Soc. London, Ser. A* **366**, 1591 (2008)
- [12] H. B. Peng *et al.*, *Phys. Rev. Lett.* **97**, 087203 (2006).
- [13] B. Lassagne *et al.*, *Nano Lett.* **8**, 3735 (2008).
- [14] K. Jensen, K. Kim, and A. Zettl, *Nature Nanotech.* **3**, 533 (2008).
- [15] H. Y. Chiu *et al.*, *Nano Lett.* **8**, 4342 (2008).
- [16] K. Jensen, H. B. Peng, and A. Zettl., *IEEE nanoscience and nanotech.* **68**, 679 (2006)
- [17] R. Lifshitz, and M. L. Roukes, *Phys. Rev. B* **61**, 5600 (2000).
- [18] D. Rugar, and P. Grutter, *Phys. Rev. Lett.* **67**, 699 (1991).
- [19] R. B. Karabalin, S. C. Masmanidis, and M. L. Roukes, *Appl. Phys. Lett.* **97**, 183101 (2010).
- [20] R. B. Karabalin, X. L. Feng, and M. L. Roukes, *Nano Lett.* **9**, 3116 (2009).
- [21] C. C. Wu, C. H. Liu, and Z. Zhong, *Nano Lett.* **10**, 1032 (2010).

- [22] M. D. Dresselhaus, G.; Avouris, Ph., *Carbon Nanotubes: Synthesis, Structure Properties and Applications* (Springer-Verlag, Berlin, 2001).
- [23] J. Kong *et al.*, *Nature* **395**, 878 (1998).
- [24] C. C. Wu. and Z. Zhong, *Nano Lett.* **11**, 1448 (2011).
- [25] V. Gouttenoire *et al.*, *Small* **6**, 1060 (2010).
- [26] V. Sazonova *et al.*, *Nature* **431**, 284 (2004).
- [27] B. Lassagne *et al.*, *Science* **325**, 1107 (2009).
- [28] D. Garcia-Sanchez *et al.*, *Phys. Rev. Lett.* **99**, 085501 (2007).
- [29] B. Witkamp, M. Poot, and H. S. J. van der Zant, *Nano Lett.* **6**, 2904 (2006).
- [30] J. S. Bunch *et al.*, *Science* **315**, 490 (2007).
- [31] A. Eichler, J. Moser, and A. Bachtold, *Nano Lett. ASAP* (2011).

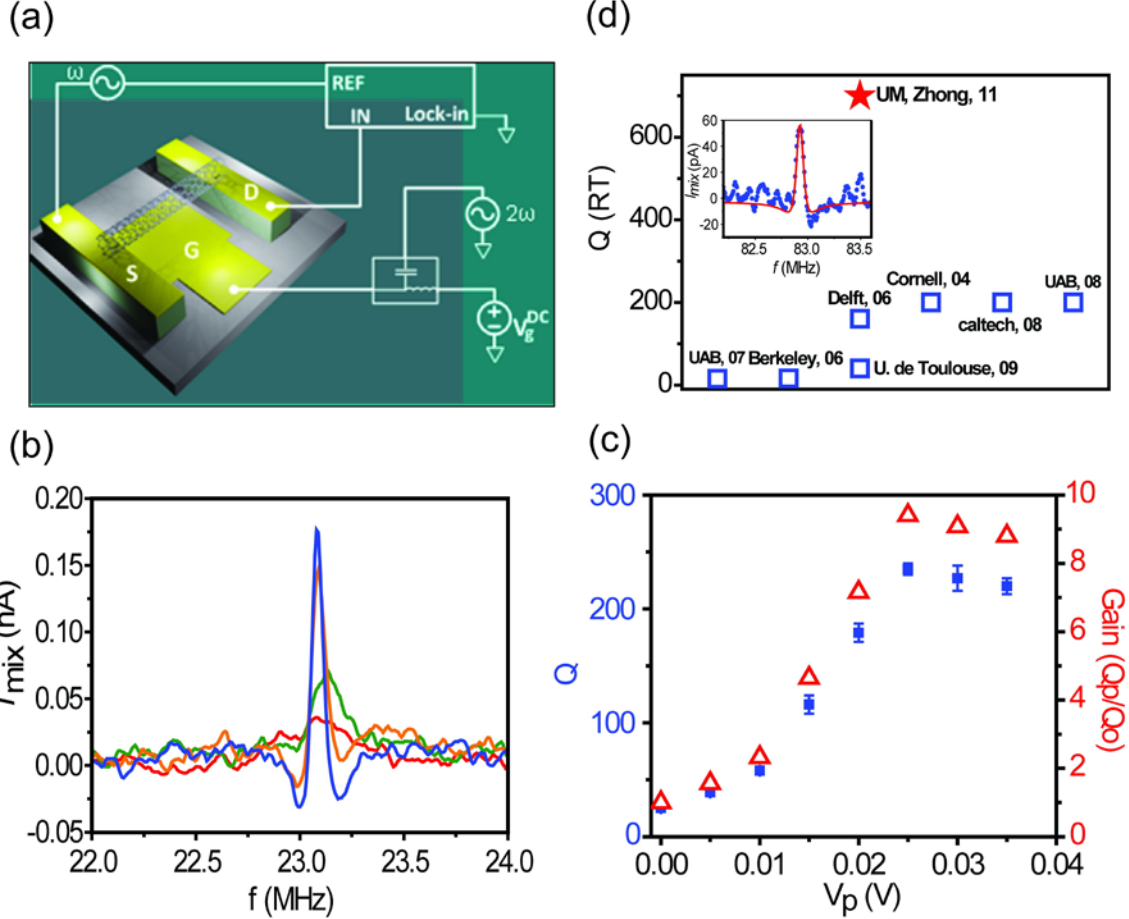


FIG. 1 (color online). (a) Schematic diagram of the experimental setup for parametric amplification in SWNT NEM resonators. (b) Frequency modulated mixing currents are plotted as a function of driving frequency at different pumping voltages ranging from 0 (red), 10 (green), 20 (orange), to 25 (blue) mV. Significant enhancement in peak current and quality factor was observed. (c) Q (blue squares) and gain (Q_p/Q_o) (red triangles) vs. V_p . The quality factor increases from 24 ± 1 ($V_p = 0$ V) to 235 ± 9 ($V_p = 25$ mV), corresponding to ~ 10 times enhancement of Q . (d) List of maximum Q 's (blue squares) reported at room temperature in previous literatures. Our maximum Q achieved through parametric amplification is around 700 (marked as star) and the resonance signal (blue dots) with fitting curve (red) is shown in the inset.

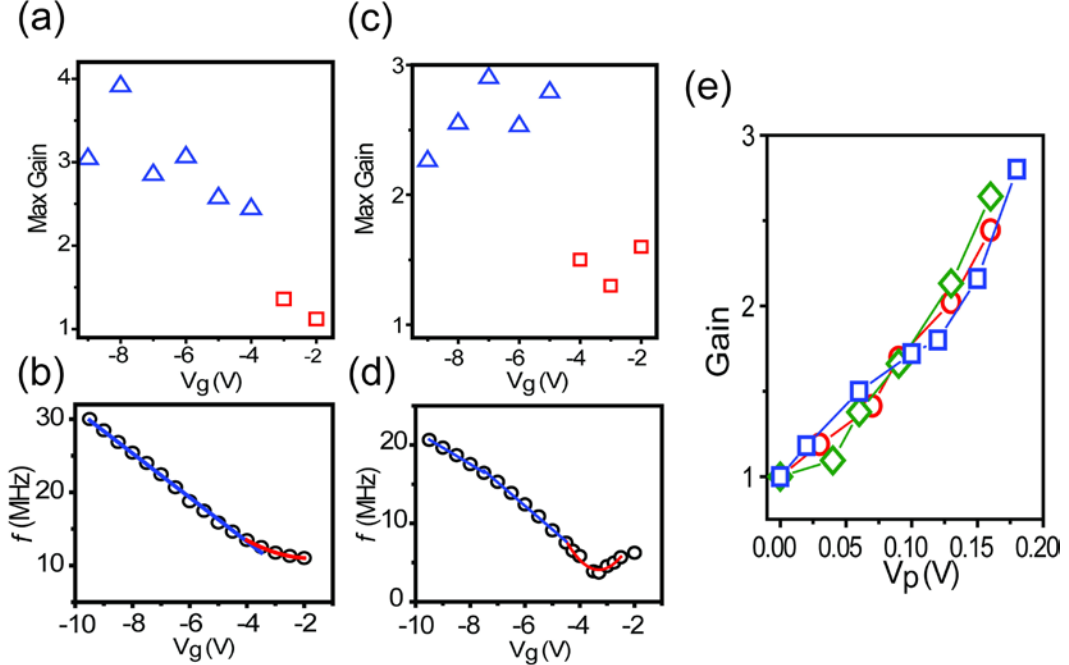


FIG. 2 (color online). (a), (c) Maximum gain vs. DC gate voltages of two SWNT resonators. The maximum gains are between 2~4 (blue triangles) in the catenary regimes but drop to 1 (red squares) in the bending regimes for both devices. (b), (d) The resonant frequency vs. DC gate voltages for two SWNT resonators. Two vibration modes, bending and catenary regimes, are shown clearly in both devices. (e) Gain vs. V_p at different driving voltages (V_{sd}) ranging from 20 (red), 40 (green) to 60 (blue) mV. No obvious dependence between gain and V_{sd} is observed.

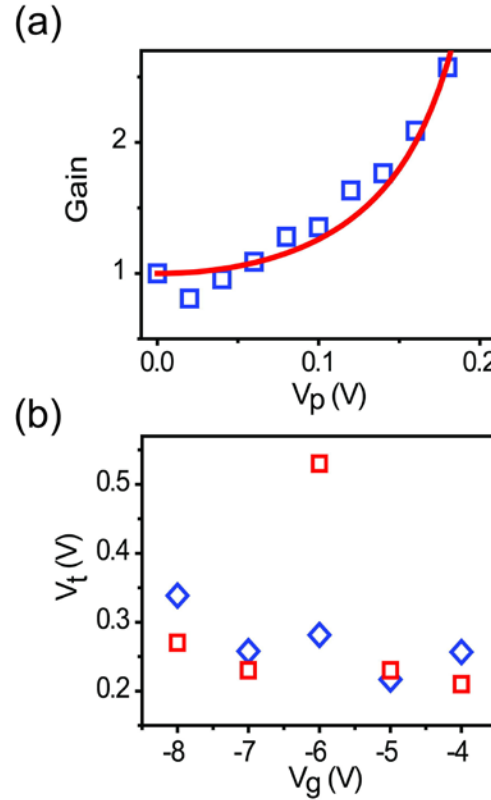


FIG. 3 (color online). (a) Gain (blue squares) vs. V_p at $V_g = -5$ V. The red curve is numerical fit by using equation (4), and $V_t = 0.24$ V is obtained. (b) Comparison of calculated V_t (blue diamonds) and measured V_t (red squares) at different gate voltages.